COMPACT DUAL-PORT HIGH-ISOLATION MIMO ANTENNA FOR WIDEBAND IOT APPLICATIONS

Abstract

For wideband internet of things (IoT) applications, this study provides a basic antenna with multiple input multiple output (MIMO) structure. To decrease the correlated coupling between the ports, a rectangular copper conductor is positioned between two antenna elements in the proposed antenna. The WLAN (2.35-2.5 GHz), WiMAX (3.2-3.85 GHz), and C band downlink (3.7-4.2 GHz) bands of Internet of Things devices are all covered by the proposed antenna's broad frequency series of 1.8-5.24 GHz. Over the whole application band, the antenna achieves a minimum port isolation of more than 20 dB. With a diversity gain (DG > 9.9 dB) and an envelope correlation coefficient (ECC < 0.002), the suggested MIMO antenna construction is highly diverse. Moreover, it has a minimum channel capacity loss (CCL) of less than 0.12 bits/s/Hz. Difference mean effective gain of two-port is less than 0.004 dB (MEG1-MEG2<0.004 dB), and total active reflection co-efficient (TARC) is better than -10 dB throughout application band.

Keywords: Compact Antenna, Mutual Coupling Reduction, Wireless Sensor Networks, Wideband MIMO, ECC, TARC, IoT.

Authors

Subhranil Samanta
Electronics and Communication Engineering Department
JIS College of Engineering
Kalyani, West Bengal, India.
subhranilsamanta92@gmail.com

Trisit Ghosh
Electronics and Communication Engineering Department
JIS College of Engineering
Kalyani, West Bengal, India.
ghoshtrisit@gmail.com

Raju Pandey
Electronics and Communication Engineering Department
National Institute of Technology
Sachar, Assam, India.
rajuece42@gmail.com

Indranath Sarkar
Electronics and Communication Engineering Department
JIS College of Engineering
Kalyani, West Bengal, India.
indranath.sarkar@jiscollege.ac.ind

Ashim Kumar Biswas
Institute of Engineering and Management (IEM), University of Engineering and Management
Kolkata, Newtown Campus, West Bengal, India.
ashim10@gmail.com

I. INTRODUCTION

In contemporary wireless communication systems, there has been a significant mandate for wideband antennas with greatest data rate [1, 2]. The on-going rapid expansion of the Internet-of-Things (IoT), pushed by purposes such as smart city, smart home, and industry 4.0, will require the connectivity of billions of objects to the internet in the near future. The enormous traffic produced by communications between things and the linkage will pose difficult problems in terms of radio contact dependability and energy consumption reduction. Now a day, the Internet of Things (IoT) becomes a technology that may link almost everything in our daily aspects. It is anticipated that the development of IoT will have a substantial impact on a number of areas of our life, such as transportation, safety, and health. IoT could be used both indoors and outdoors in daily life, which is why there is a growing need for antenna designs that can blend in seamlessly with a variety of items [3-5]. Widespread promises in wireless communication are made about multiple-input multiple-output (MIMO) systems, which are said to improve system reliability, signal quality, and data throughput [6-8]. Hills or big structures in a wireless communication setting might cause multipath fading of the transmitted signal. In order to reduce multipath fading and increase system capability, multiple-input multiple-output (MIMO) arrangements are frequently employed in wireless communication [9, 10]. A MIMO system has several antennas on both the transmitter and receiver sides. Thus, in compact devices, closely spaced antennas lead to substantial mutual coupling between the antenna elements and result in limited channel capacity distorted radiation patterns [11-13].

The literature on wireless MIMO system applications reports several MIMO antenna designs with decreased mutual coupling. A 66 mm × 32 mm × 1.5 mm antenna with an operating frequency variety of 1.5-5.1 GHz is proposed in Ref. [14]. To achieve more than 15 dB port isolation, it makes advantage of several vertical slots in the ground plane. Ref. [15] describes a two-element MIMO structure comprises a least port-isolation of 9 dB that operates in the 1.71- 1.88 GHz and 2.5-2.7 GHz frequency ranges. A slot-based MIMO antenna involving the 2.4-2.5 GHz and 4.9–5.725 GHz multiband characteristics is shown in Reference [16]. That article states that the maximum port isolation is around 18 dB.

An IoT antenna's precise specifications have not yet been decided upon. The performance of the antenna is crucial to this technology and directly contributes to the IoT environment's rapid development. These days, the most common IoT applications include security, tracking, agriculture, smart cities, and smart homes. Therefore, proposed designed MIMO antenna is very important and can be suitable to implement with an IoT device.

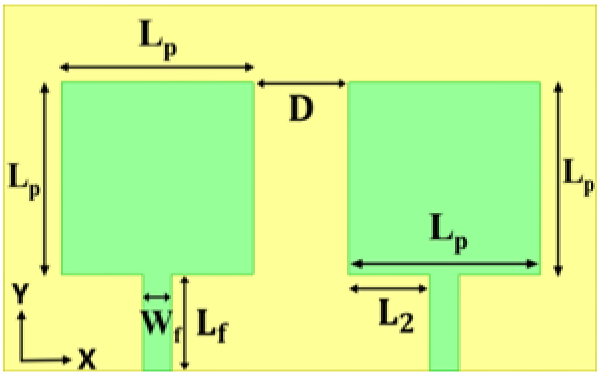

(A)

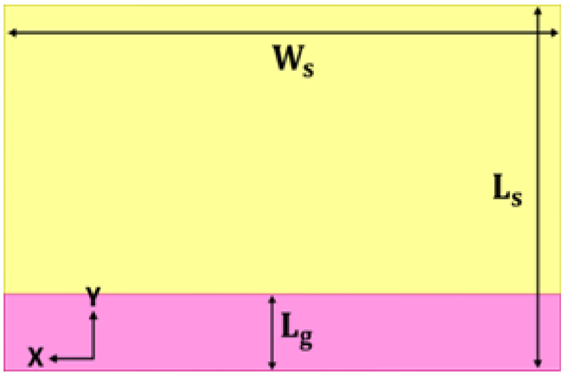

(B)

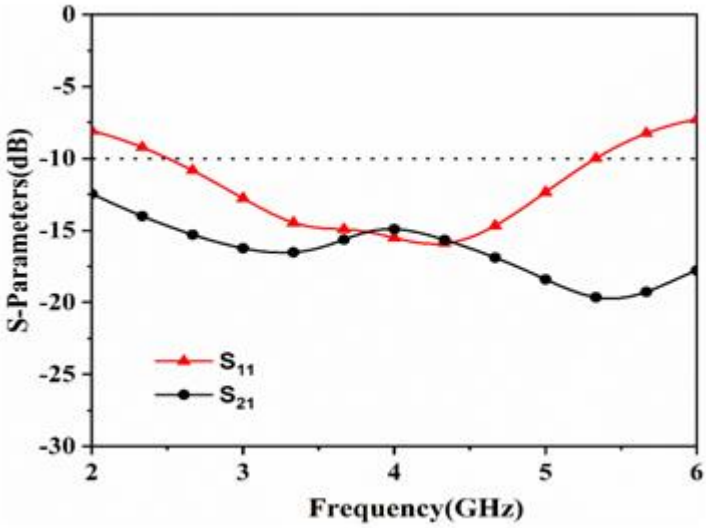

(C)

Figure 1: MIMO antenna without Copper conductor (A) top view, (B) bottom view, (C) S-Parameters

II. ANTENNA DESIGN AND RESULTS

The antenna, having a dielectric constant (ε_r) of 4.4 along with a loss tangent (tan δ) of 0.024, is integrated into a FR4 epoxy substrate. The antenna measures 62 mm × 38 mm × 1.6 mm in its total dimensions. The suggested MIMO system, located on upper surface of the substrate, consists of two square-shaped patches spaced 10 mm apart. The antenna elements on upper side of the substrate are connected by a very basic copper cable in order to minimize mutual interaction between them. The dimensions of the suggested MIMO antenna are shown in Table 1.

1. Mimo Structure Without Copper Conductor

Figure 1 depicts a dual-element MIMO antenna devoid of a copper wire. Both antenna elements' feeding structures and port positions are shown in the upper layer (Figure 1A). In Figure 1B, the ground plane is displayed at the bottom. Figure 1C shows the S-parameters for the antenna, which is simulated using Ansys HFSS [17]. Operating in the $S_{11} \leq$-10 dB frequency spectrum, the antenna provides poor port isolation (S_{21} (dB)) and operates in the 2.51 to 5.31 GHz range.

2. Mimo Antenna with Copper Conductor

Figure 2 depicts a copper-conducted dual-element MIMO antenna. The copper conductor, positioned in between the two antenna elements, is visible in the upper layer (Figure 2A). The bottom layer (Figure 2B) shows the ground plane, which is the same size as the MIMO antenna but does not have a copper wire. Ansys HFSS is used to model the antenna, and figure 2 C displays the S-parameters. With port isolation (S_{21}(dB)) reaching more than 20 dB over the broad frequency band of 2.35 to 4.2 GHz, the antenna operates in the frequency range of 1.8 to 5.24 GHz (S11 ≤-10 dB).

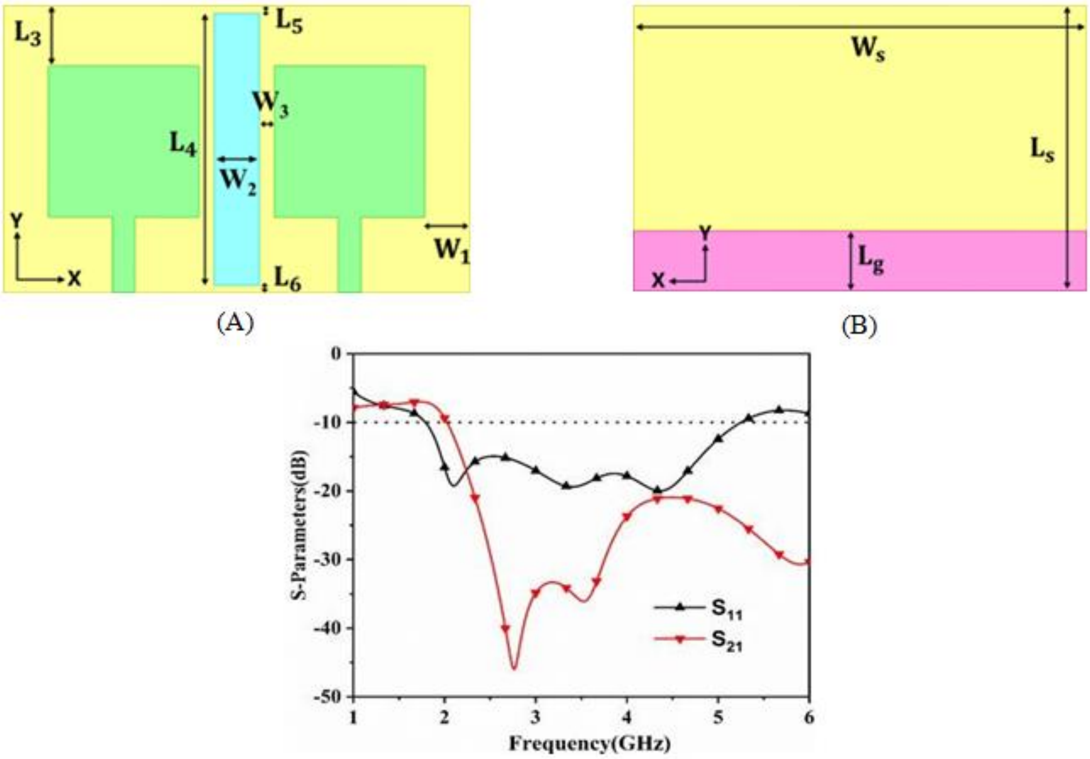

Figure 2: MIMO antenna with Copper conductor on top surface- (A) topmost view, (B) bottommost view, (C) S- Parameters

Table 1: Parameter-wise dimensions of the MIMO antenna

Parameter	Dimension (mm)	Parameter	Dimension (mm)	Parameter	Dimension (mm)
L_p	20	L_2	8.5	L_3	8
L_4	36	L_5	1	L_6	1
L_S	38	L_f	10	L_g	8
W_1	6	W_2	6	W_3	2
W_s	62	W_f	3	D	10

III. SURFACE CURRENT DISTRIBUTIONS

Figure 3 shows the simulations of the surface current circulations at 2.4 GHz and 3.5 GHz with and without a copper conductor. The effectiveness with which the antenna with copper conductor lowers mutual coupling between antenna ports is demonstrated in Figure 3. In comparison to an antenna without a copper conductor, the surface current distributions show that the current coupling from the input excitation port 1 to port 2 in the copper conductor antenna is less. The copper conductor prevents the near-field radiation from the antenna between the two radiating elements by preventing the current commencing from port 1 inflowing to port 2.

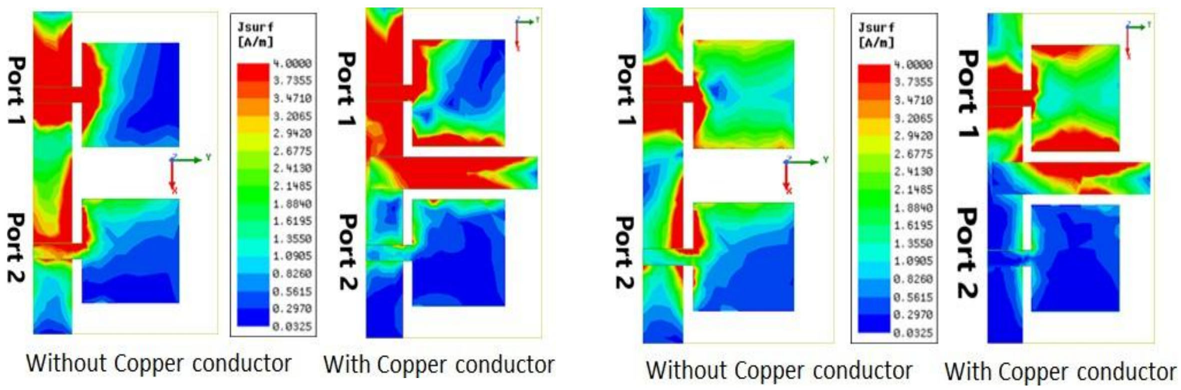

(A) (B)

Figure 3: Surface current representations at- (A) 2.4 GHz; (B) 3.5 GHz

IV. RADIATION PROPERTIES

Figure 4A-B displays the simulated radiation schemes of the planned MIMO antenna in the E-plane at 2.4 GHz and the H-plane at 4.2 GHz. Figure 5 clarifies how the gain varies with the suggested antenna's frequency. Gains are progressively raised in proportion to frequency, peaking at 3.038 dB at 4.75 GHz. Moreover, a gain of 0.4 dB at 2.4 GHz and 2.48 dB at 4.2 GHz is noted.

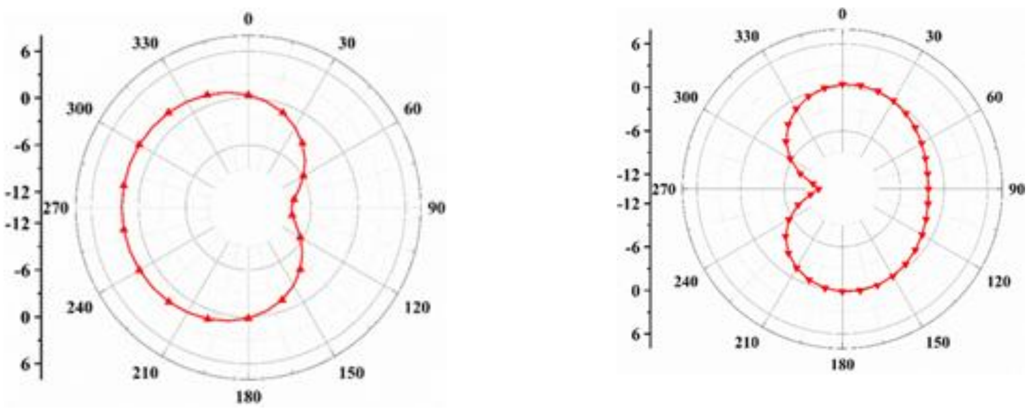

E-Plane H-Plane

(A)

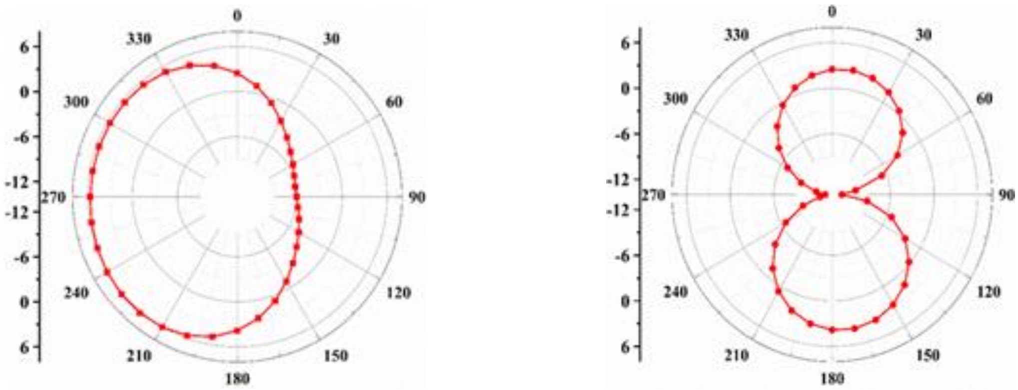

E-Plane H-Plane

(B)

Figure 4: Radiation schemes at (A) 2.4 GHz, (B) 4.2 GHz

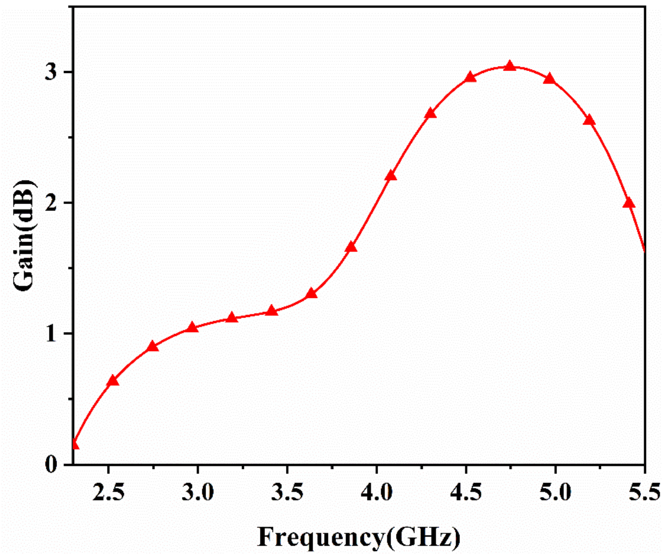

Figure 5: Variation of Gain vs Frequency of the proposed antenna

V. DIVERSITY PRESENTATIONS

Through the computation of metrics of different diversity parameters ensure the practicality of the MIMO characteristics. Therefore, these parameters are included to evaluate the designed antenna. The assessment clarifies the suitability of projected MIMO structure's diversity enactment [18].

1. Envelope Correlation Coefficient (ECC)

Radiation patterns or S-parameters can be utilized to calculate the ECC parameter, which is used to find the correlation between antenna elements. For the majority of MIMO antenna designs, the ideal ECC value is less than 0.4. However, any value below that is not recommended for optimal diversity performance. Equation 1 can be used to calculate the ECC of a dual-port MIMO system [19, 20].

$$ECC = \frac{|S_{aa}^{*}S_{ab} + S_{ba}^{*}S_{bb}|^2}{(1-|S_{aa}|^2 - |S_{ba}|^2)(1-|S_{bb}|^2 - |S_{ab}|^2)} \quad (1)$$

Subscripts a, b denote port numbers. It is perceived from the figure 6, ECC < 0.002 throughout the whole application band of the MIMO antenna.

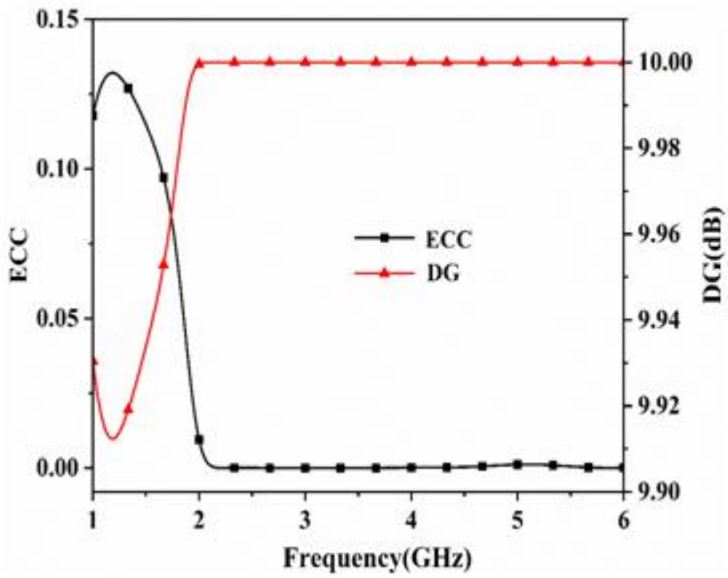

Figure 6: ECC and DG of the suggested antenna

2. Diversity Gain (DG)

To further examine the MIMO diversity performance, the DG is another essential metric. The diversity gain and the ECC are strongly correlated since the greater the diversity gain, lesser the correlation between the antenna elements, and vice versa. Equation 2 allows for the computation of the DG from the envelope correlation coefficient (ECC) [21].

$$DG = 10\sqrt{1-(ECC)^2} \quad (2)$$

Figure 6 shows a much appreciated diversity gain (DG > 9.9 dB) over the complete claimed frequency bands for the planned MIMO antenna.

3. Channel Capacity Loss (CCL)

If the MIMO system has more antenna components, channel capacity can be increased; however, CCL is caused by the correlation between closely spaced antenna elements. For dependable communication, a MIMO antenna system's CCL have to be less than 0.4 bits/sec/Hz. Equation 3 [22-23] may be used to calculate this CCL.

$$C(Loss) = -\log_2 \det(\psi^R) \quad (3)$$

where ψ^R denotes receiver end antenna correlation matrix. In lieu of two element MIMO system, ψ^R is a 2×2 correlation matrix and it is expressed as

$$\Psi^R = \begin{bmatrix} \rho_{11} & \rho_{12} \\ \rho_{21} & \rho_{22} \end{bmatrix}, \ \rho_{ii} = 1 - (|S_{ii}|^2 + |S_{ij}|^2)$$

Here $\rho_{ij} = -(S_{ii}^* S_{ij} + S_{ji}^* S_{ij})$, and i, j are 1 or 2.

Figure 7(A) shows the channel capacity loss lies below 0.11 Bit/s/Hz (threshold value is 0.4 Bit/s/ Hz) throughout the entire application band.

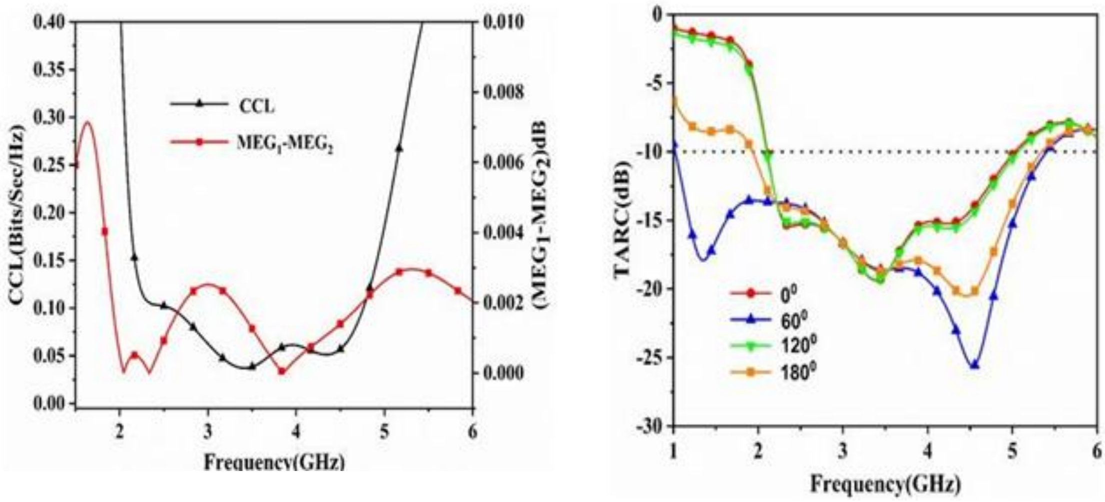

(A) (B)

Figure 7: (A) CCL and MEG of the proposed antenna, (B) TARC of the proposed antenna

4. Mean Effective Gain (MEG)

The mean effective gain is a fundamental diversity parameter (MEG). MEG aids in the explanation of the antenna's performance in relation to its gain and environmental impact. By utilizing S-parameters from the following equation 4 [24], one can ascertain the MEG of both antenna ports k, y.

$$MEG_i = 0.5\eta_{k,rad} = 0.5(1 - \sum_{y=1}^{N} |S_{ky}|^2) \tag{4}$$

Figure 7(A) shows that the variance between two MEGs is less than 0.004 dB all through the operational band, representing the typical choice of a MIMO antenna.

5. Total Active Reflection Coefficients (TARC)

The square root of the total reflecting energy dividing by the square root of total incident energy is known as TARC [25]. TARC is defined as the total return loss of the MIMO antenna system and may be calculated using equation 5 [26].

$$\Gamma = \frac{\sqrt{\left(|(S_{11} + S_{12}\, e^{j\theta})|^2 + |(S_{21} + S_{22}\, e^{j\theta})|^2\right)}}{\sqrt{2}} \tag{5}$$

The phase difference between ports 1 and 2 ranges from 0 to 180 degree with an incremental size of 60 degree. Figure 7(B) demonstrates that the TARC value is greater than -10 dB for all values of across the application band. A comparative study is done with similar works in TABLE 2.

Table 2: Comparative assessment of the proposed design with some of the related works

Ref.	**Antenna size (mm^3), Ports**	**Gain**	**ECC**	**CCL (bits/sec/Hz**	**Bandwidth (GHz)**	**Isolation (dB)**
[6]	50×110×1.56, 4	-0.6 dBi	0.16	Not shown	1.73-2.28	10
[9]	55 × 35 × 1.5, 2	6.9 dB	0.025	0.13	3.1-10.6	26
[10]	π × 15 × 2, 2	6 dB	0.18	0.24	7.96-8.76	21
[16]	46 × 20 × 1.6, 2	2.9 dBi	0.2	Not shown	2.4-2.5, 4.9-5.725	14
[24]	50 × 50 × 14.6, 2	5.1 dB	0.05	04	3.1-3.7	25
[26]	32 × 52 × 2, 2	3 dB	0.09	0.33	2.22-8	20
Prop.	62 × 38 × 1.6, 2	3 dB Peak	0.002	0.12	1.8-5.24	20

VI. CONCLUSIONS

This communication presents a dual-port MIMO antenna for IoT device with high port isolation. A copper conductor in the middle of antenna elements is arranged at the uppermost area of the substrate. It compromises more than 20 dB isolation in the 2.35 -4.2 GHz band for the considered antenna. The antenna offers very low envelope correlation coefficient (ECC < 0.002), high Diversity Gain (DG > 9.9dB) low channel capacity loss (CCL < 0.12 Bit/s/Hz), low difference MEG (MEG1-MEG2<0.004dB) and TARC value better than -10dB correspondingly. The antenna covers a size of 62 × 38 mm^2 with an element spacing distance of 10 mm. The antenna can be fabricated and measured outcomes may be utilized to compare the simulated outcomes. However, simulated results from Ansys HFSS are very close to the measured results.

REFERENCES

[1] R. Hussain, M.S. Sharawi and A. Shamim, "An integrated four-element slot-based MIMO and a UWB sensing antenna system for CR platforms," *IEEE Transactions on Antennas and Propagation, 66*(2), pp. 978-983, 2017.

[2] U. Chakraborty, A. K Biswas, S. Maity, B. Roy, S. Roy, "Dielectric resonator array antenna for triple band WLAN applications with enhanced gain," International Journal of RF and Microwave Computer-Aided Engineering, 29(2), pp. e21529, 2019. Doi: https://doi.org/10.1002/mmce.21529

[3] J. I. Oh, H. W. Jo, K. S. Kim, H. Cho and J. W. Yu, "A Compact Cavity-Backed Slot Antenna Using Dual Mode for IoT Applications," *IEEE Antennas and Wireless Propagation Letters*, vol. 20, no. 3, pp. 317-321, March 2021, doi: 10.1109/LAWP.2021.3049219.

[4] A. Zandamela, A. Chiumento, N. Marchetti, M. J. Ammann and A. Narbudowicz, "Exploiting Multimode Antennas for MIMO and AoA Estimation in Size-Constrained IoT Devices," in IEEE Sensors Letters, vol. 7, no. 3, pp. 1-4, March 2023, Art no. 5500904, doi: 10.1109/LSENS.2023.3244870

[5] M. A. S. Sejan and W. -Y. Chung, "Performance Analysis of a Long-Range MIMO VLC System for Indoor IoT," in IEEE Internet of Things Journal, vol. 10, no. 8, pp. 6999-7010, 15 April15, 2023, doi: 10.1109/JIOT.2022.3228555.

[6] R. Hussain, M.U. Khan and M.S. Sharawi, 2017. An integrated dual MIMO antenna system with dual-function GND-plane frequency-agile antenna. *IEEE Antennas and Wireless Propagation Letters*, *17*(1), pp.142-145.

[7] A. K. Biswas, S. Biswas, S. Haldar, A. Nandi, "A Highly Decoupled Flexible 4-element MIMO Antenna with Band Notched Characteristics for Ultra Wide-band Wearable Applications," AEU - International Journal of Electronics and Communications, 173, pp. 154985, 2024.

[8] W. Hu *et al*., "Dual-Band Antenna Pair With High Isolation Using Multiple Orthogonal Modes for 5G Smartphones," IEEE Transactions on Antennas and Propagation, vol. 71, no. 2, pp. 1949-1954, Feb. 2023, doi: 10.1109/TAP.2022.3233458.

[9] A.K. Biswas and U. Chakraborty, 2019. Compact wearable MIMO antenna with improved port isolation for ultra-wideband applications. *IET Microwaves, Antennas & Propagation*, *13*(4), pp.498- 504.

[10] A. K. Biswas, S. S. Pattanayak, U. Chakraborty, "Evaluation of Dielectric Properties of Colored Resin Plastic Button to Design a Small MIMO Antenna," IEEE Transactions on Instrumentation and Measurement, 69(11), 9170 – 9177, 2020.

[11] S. Zuo, Y.Z. Yin, W.J. Wu, Z.Y. Zhang and J. Ma, 2010. Investigations of reduction of mutual coupling between two planar monopoles using two λ/4 slots. *Progress In Electromagnetics Research Letters*, *19*, pp.9-18.

[12] A. K. Biswas and U. Chakraborty, "A compact single element dielectric resonator MIMO antenna with low mutual coupling," *Frequenz*, vol. 75, no. 5-6, 2021, pp. 201-209. https://doi.org/10.1515/freq-2020-0167

[13] Y. Fang, Y. Jia, J. Q. Zhu, Y. Liu and J. An, "Self-Decoupling, Shared-Aperture, Eight-Antenna MIMO Array With MIMO-SAR Reduction," in IEEE Transactions on Antennas and Propagation, vol. 72, no. 2, pp. 1905-1910, Feb. 2024, doi: 10.1109/TAP.2023.3339223.

[14] H.T. Hu, F.C. Chen and Q.X Chu, 2015. A wideband U-shaped slot antenna and its application in MIMO terminals. *IEEE Antennas and Wireless Propagation Letters*, *15*, pp.508-511.

[15] A.N. Kulkarni and S.K. Sharma, 2012. Frequency reconfigurable microstrip loop antenna covering LTE bands with MIMO implementation and wideband microstrip slot antenna all for portable wireless DTV media player. *IEEE Transactions on antennas and propagation*, *61*(2), pp.964-968.

[16] S. Soltani, P. Lotfi and R.D. Murch, 2016. A port and frequency reconfigurable MIMO slot antenna for WLAN applications. *IEEE Transactions on Antennas and Propagation*, *64*(4), pp.1209-1217.\

[17] HFSS ver.18, Ansys Corporation. Pittsburgh, PA, USA.

[18] A.K. Biswas and U. Chakraborty, 2019. Reduced mutual coupling of compact MIMO antenna designed for WLAN and WiMAX applications. *International Journal of RF and Microwave Computer-Aided Engineering*, *29*(3), p.e21629.

[19] S Blanch, J Romeu and I. Corbella, 2003. Exact representation of antenna system diversity performance from input parameter description. Electron Lett, 39(9):705-707.

[20] R. Pandey, A. K. Biswas, U. Chakraborty, "Compact body-worn MIMO antenna with high port isolation for UWB applications," International Journal of Communication Systems, e5764, DOI: https://doi.org/10.1002/dac.5764

[21] A.K. Biswas and U. Chakraborty, 2019. Investigation on decoupling of wide band wearable multiple-input multiple-output antenna elements using microstrip neutralization line. *International Journal of RF and Microwave Computer-Aided Engineering*, *29*(7), p.e21723.

[22] Y.K. Choukiker, S.K. Sharma and S.K., Behera, 2013. Hybrid fractal shape planar monopole antenna covering multiband wireless communications with MIMO implementation for handheld mobile devices. *IEEE Transactions on Antennas and Propagation*, *62*(3), pp.1483-1488.

[23] S. Roy, A. K. Biswas, S. Ghosh, U. Chakraborty, A. Sarkhel, "Isolation improvement of dual-/quad-element textile MIMO antenna for 5G application," Journal of Electromagnetic Waves and Application, 35(10), 1337-1353, 2021.

[24] G. Das, A. Sharma and R.K. Gangwar, 2017. Dual port aperture coupled MIMO cylindrical dielectric resonator antenna with high isolation for WiMAX application. *International Journal of RF and Microwave Computer-Aided Engineering*, *27*(7), p.e21107.

[25] A.K. Biswas and U. Chakraborty, 2019. A compact wide band textile MIMO antenna with very low mutual coupling for wearable applications. *International Journal of RF and Microwave Computer- Aided Engineering*, *29*(8), p.e21769.

[26] R. Pandey, A. K. Biswas, U. Chakraborty, "Non-conventional leather substrate based high isolation wideband MIMO antenna for body-centric applications," *AEU-International Journal of Electronics and Communications*, vol. 170, 154871 (2023), https://doi.org/10.1016/j.aeue.2023.154871

[27] B. A. Esmail, S. Koziel, "High isolation metamaterial-based dual-band MIMO antenna for 5G millimeter-wave applications," AEU - International Journal of Electronics and Communications, vol. 158, 154470, 2023, https://doi.org/10.1016/j.aeue.2022.154470.